

Received: 2017.04.22

Accepted: 2017.05.11

Published: 2017.05.31

# Granulocyte-Colony Stimulating Factor (G-CSF) Accelerates Wound Healing in Hemorrhagic Shock Rats by Enhancing Angiogenesis and Attenuating Apoptosis

Authors' Contribution:  
Study Design A  
Data Collection B  
Statistical Analysis C  
Data Interpretation D  
Manuscript Preparation E  
Literature Search F  
Funds Collection G

ABCDEF 1,2,3 **Hong Huang\***  
BCF 1,2,3 **Qi Zhang\***  
BCF 1,2 **Jiejie Liu**  
AE 1,2 **Haojie Hao**  
AEF 1,2 **Chaoguang Jiang**  
AFG 1,2 **Weidong Han**

1 Department of Molecular and Immunological, Chinese PLA General Hospital, Beijing, P.R. China  
2 Department of Bio-Therapeutic, Chinese PLA General Hospital, Beijing, P.R. China  
3 Medical school of Nankai University, Tianjin, P.R. China

\* These authors contributed equally to this study

**Corresponding Author:** Weidong Han, e-mail: [hanwdrsw69@yahoo.com](mailto:hanwdrsw69@yahoo.com)

**Source of support:** This study was supported by the National Basic Science and Development Program [2012CB518103], the 863 Projects of Ministry of Science and Technology of China [2013AA020105 and 2012AA020502]

**Background:** Following severe trauma, treatment of cutaneous injuries is often delayed by inadequate blood supply. The aim of the present study was to determine whether granulocyte-colony stimulating factor (G-CSF) protects endothelial cells (ECs) and enhances angiogenesis in a rat model of hemorrhagic shock (HS) combined with cutaneous injury after resuscitation.

**Material/Methods:** The HS rats with full-thickness defects were resuscitated and randomly divided into a G-CSF group (200 µg/kg body weight), a normal saline group, and a blank control group. Histological staining was used to estimate the recovery and apoptosis of skin. Apoptosis- and angiogenesis-related factors were analyzed by reverse transcription-polymerase chain reaction (RT-PCR) and Western blot (WB). Scratch assay, tube formation, and WB experiments were performed to verify the functional effects of G-CSF on HUVECs *in vitro*.

**Results:** H&E staining and Masson trichrome staining showed earlier inflammation resolution and collagen synthesis in the G-CSF-treated group. Angiogenesis-related factors were elevated at mRNA and protein levels. TUNEL staining suggested fewer apoptotic cells in the G-CSF group. The apoptotic-related factors were down-regulated and anti-apoptotic factors were up-regulated in the G-CSF-treated group. Scratch assay and tube formation experiments revealed that G-CSF facilitated migration ability and angiogenic potential of HUVECs. The angiogenic and anti-apoptotic effects were also enhanced *in vitro*.

**Conclusions:** Our results suggest that G-CSF after resuscitation attenuates local apoptosis and accelerates angiogenesis. These findings hold great promise for improving therapy for cutaneous injury in severe trauma and ischemia diseases.

**MeSH Keywords:** **Angiogenesis Modulating Agents • Apoptosis • Endothelial Cells • Receptors, Granulocyte Colony-Stimulating Factor**

**Full-text PDF:** <http://www.medscimonit.com/abstract/index/idArt/904988>

 2441  1  4  36



## Background

Traumatic hemorrhagic shock (THS) is a life-threatening condition. Without proper control, it can lead to multiple organ damage syndrome (MODS) and even death. In our previous study, we demonstrated that resuscitation and G-CSF treatment accelerate wound repair in hemorrhagic shock. The present study was focused on the protective mechanisms of G-CSF after resuscitation treatment in a rat model of cutaneous injury combined with hemorrhagic shock.

Wound healing consists of well-orchestrated processes, including inflammation, proliferation and maturation, and successive remodeling phases [1,2]. However, skin injuries are affected by other severe trauma in traffic accidents or war injuries, which easily develop into non-healing wounds [3,4]. Although combined injuries like hemorrhagic shock combined with cutaneous injury often occur in traffic accidents and war, little is known about wounds affected by blood loss and the wound repair process. The restriction of blood supply to skin after blood loss leads to tissue hypoxia and even tissue necrosis [5–7]. Severe blood supply inefficiency and tissue apoptosis hinder wound repair because of endothelial cell (ECs) dysfunction in injured tissues [8].

G-CSF, a hematopoietic cytokine and potent stem cell mobilization agent, has been applied in preclinical as well as clinical therapies [9–11]. G-CSF showed its angiogenesis property in endothelial cells (ECs) *in vivo* and *in vitro* [12–14], and ECs were reported to actively proliferate and form vascular-like structures in response to G-CSF [15]. Consequently, G-CSF treatment had been considered as an alternative approach for angiogenesis therapy [16,17]. Recently, increasing evidence suggested that G-CSF has tissue-protective roles through enhancing anti-apoptotic and anti-inflammatory capabilities of the host cells [18–22]. However, the effects on ECs in hemorrhagic shock combined with cutaneous injury have not been elucidated. In this study, we aimed to determine if G-CSF would benefit wound repair by accelerating angiogenesis and anti-apoptotic abilities of ECs in hemorrhagic shock.

G-CSF has been proved to promote tissue repair and regeneration in many injuries. In the present study, we applied a rat model of hemorrhagic shock combined with cutaneous injury. We found that G-CSF injection after resuscitation accelerated wound repair progression by stimulating angiogenesis and promoting early anti-apoptotic capacities. *In vitro* experiments showed that G-CSF increased the migration and tube formation and enhanced the anti-apoptotic abilities of HUVECs.

## Material and Methods

### Experimental animals

A total of 54 male SD rats (250–300 g) were obtained from the Experimental Animal Department of the Chinese PLA General Hospital. All animal procedures in this study were conducted in accordance with the guidelines of the Institutional Animal Care Committee of the Chinese PLA General Hospital and were carried out in accordance with the guidelines of the China Council on Animal Care and Use (Approval ID: 2013022089). All surgeries and measurements were performed under sodium pentobarbital anesthesia and we tried to minimize suffering. The animals were kept under standard pathogen-free conditions, with  $25\pm 1^\circ\text{C}$  room temperature, humidity  $50\pm 5\%$  12-h light/dark cycles, in individual cages, and fed pellet diet and water *ad libitum*.

### Animal model

The hemorrhagic shock combined with cutaneous injury model was established as previously described [23]. Briefly, the SD rats were anesthetized with sodium pentobarbital (40 mg/kg), and a supplement was given during the experiment. First, a full-thickness, 3-cm, circular excision wound was made after shaving the targeted dorsal fur and disinfection with iodophor. Wounds were dressed with sterile gauze held in place by elastic bandages. The dressings were wetted by normal saline and removed 3 days after injury. Controlled hemorrhagic shock was induced by withdrawing 40% of the total blood volume from the carotid artery during 1 h. All the rats received hypertonic saline solution resuscitation (4 mL/kg body weight, 7.2% NaCl/6% hydroxyethyl starch, Fresenius Company, Germany), followed by reinfusing half of the withdrawn blood. Then, all the rats were randomly divided into 3 groups: in the G-CSF group ( $n=18$ ), G-CSF was subcutaneously administered (200  $\mu\text{g}/\text{kg}$ , Kyowa Hakko Kirin, Japan) for 3 consecutive days; and the control groups received an equal dose of normal saline (normal saline group,  $n=18$ ) for 3 days or not (blank group,  $n=18$ ), separately. All surgical procedures were performed under sterile conditions.

### H&E staining and Masson Trichrome staining

At indicated timepoints after injury, the rats were killed by overdose sodium pentobarbital injection and the wounded skins were harvested for further analysis. The wound tissues were fixed with formaldehyde solution for at least 48 h and then embedded in paraffin. The sections (6- $\mu\text{m}$ ) were dewaxed in a graded xylene series, followed by standard H&E and Masson trichrome staining to reveal the morphology and collagen deposition during the wound recovery process. The specimens were photographed using a light microscope (Leica TCS SP2, Germany).

**Table 1.** Primers used in qRT-PCR.

Primers	Temperature	Sequences	Length
IL4	55°C	Forward TGATGTACCTCCGTGCTTGA	197 bp
		Reverse AGGACATGGAAGTGCAGGAC	
CD31	55°C	Forward ATGGCCAGAAATCAAGGAGC	169 bp
		Reverse ACCTCAAGCAAAGCAAAGA	
Col I	55°C	Forward GACGGCTGGAGGAGAGTTC	123 bp
		Reverse CTGGTGAACGTGGTGACG	
α-SMA	55°C	Forward AGGGAGTGATGGTTGGAATG	107 bp
		Reverse GATGATGCCGTGTTCTATCG	
HGF	55°C	Forward CATTGGTAAAGGAGGCAGCTATAAA	253 bp
		Reverse GGATTCGACAGTAGTTTTCTGTAGG	
Bcl 2	56°C	Forward TTCGGGATGGAGTAAACTGG	150 bp
		Reverse AAGGCTCTAGGTGGTCATTGAC	
β-actin	56°C	Forward GAGAGGGAAATCGTGCCTGAC	580 bp
		Reverse CATCTGCTGGAAGGTGGACA	

Col I – collagen I; HGF – hepatocyte growth factor.

### TUNEL assay

The tissue apoptosis was evaluated by use of an *in situ* TUNEL kit (Promega, USA) according to the manufacturer's instructions. The paraffin-embedded skin tissue sections were deparaffinized and rehydrated and treated by proteinase K. Then, the sections were incubated with a nucleotide mixture containing fluorescein 12-UTP and TDT. The sections were visualized using 3'-diaminobenzidine tetrahydrochloride (DAB) solution (TIANGEN, China). The positively stained cells were counted under an inverted phase-contrast microscope (Leica, Germany).

### Real-time PCR (RT-PCR)

The cDNA of each sample was synthesized by a RevertAid™ First Strand cDNA Synthesis Kit (Thermo Fisher Scientific, USA) from 3 µg of total RNA. The relative mRNA expression was quantified by RT-PCR using SYBR green qPCR Mix (TOYOBO, Japan). RT-PCR was performed on an ABI PRISM 7500 device (Applied Biosystems, USA). The primers used are listed in Table 1. Each experiment was performed in triplicate. The relative gene expression was normalized by β-actin and calculated using ABI PRISM 7500 v. 2.0.6 software (Applied Biosystems, USA) with the  $2^{-\Delta\Delta Ct}$  method.

### Cell migration and tube formation assay.

To examine the effect of G-CSF on HUVECs migration, the migration and tube formation abilities of the endothelial cells were assessed. The HUVECs were seeded on a 24-well plate.

The original wounds were inflicted by dragging a sterile pipette tip across the monolayer, creating 350-µm cell-free paths. The medium was then added separately to different concentrations of G-CSF at 0.5, 5, 50, 500, and 1000 ng/mL for 12 h. The vascular tube formation assay was performed by seeding the HUVECs in a 24-well plate precoated with Matrigel™ (BD, Germany), adding different concentrations of G-CSF and incubating the plates for 12 h at 37°C. The number of capillary-like structures was quantified and visualized under an inverted phase-contrast microscope (Leica, Germany).

### Western blotting

For tissue protein extraction, skin tissues were frozen and then ground in tissue lysis buffer. For cell protein extraction, the HUVECs were cultured on a 6-well plate and pretreated with G-CSF in different concentrations for 24 h and followed by H<sub>2</sub>O<sub>2</sub> (50 µmol/L) treatment for 6 h, then the cells were lysed and total protein was harvested. The proteins were separated by 12% SDS-PAGE and then electroblotted by PVDF membranes. The blots were blocked for 1 h in 5% nonfat dry milk, and the first antibodies were added at the following proper dilutions and kept overnight at 4°C: pAKT antibody (1: 1500, CST technology, USA), AKT antibody (1: 1500, CST technology), VEGF (1: 1000, Abcam, USA), α-SMA (1: 500, BOSTER, China), collagen I (1: 500, BOSTER), Bcl 2 (1: 1000, CST technology), caspase 3 (1: 1500, CST technology), and mouse monoclonal β-actin antibody (1: 4000, Santa Cruz, USA). The blots were incubated with HRP-conjugated secondary antibody at 1: 3000 (Santa Cruz) for

50 min at room temperature using an orbital shaker. Finally, the bands were visualized using a SuperSignal West Pico chemiluminescent substrate (Thermo Fisher Scientific) and exposed on X-ray images.  $\beta$ -actin was loaded as an internal control and protein expressions were quantified by use of Image J software.

### Statistical analysis

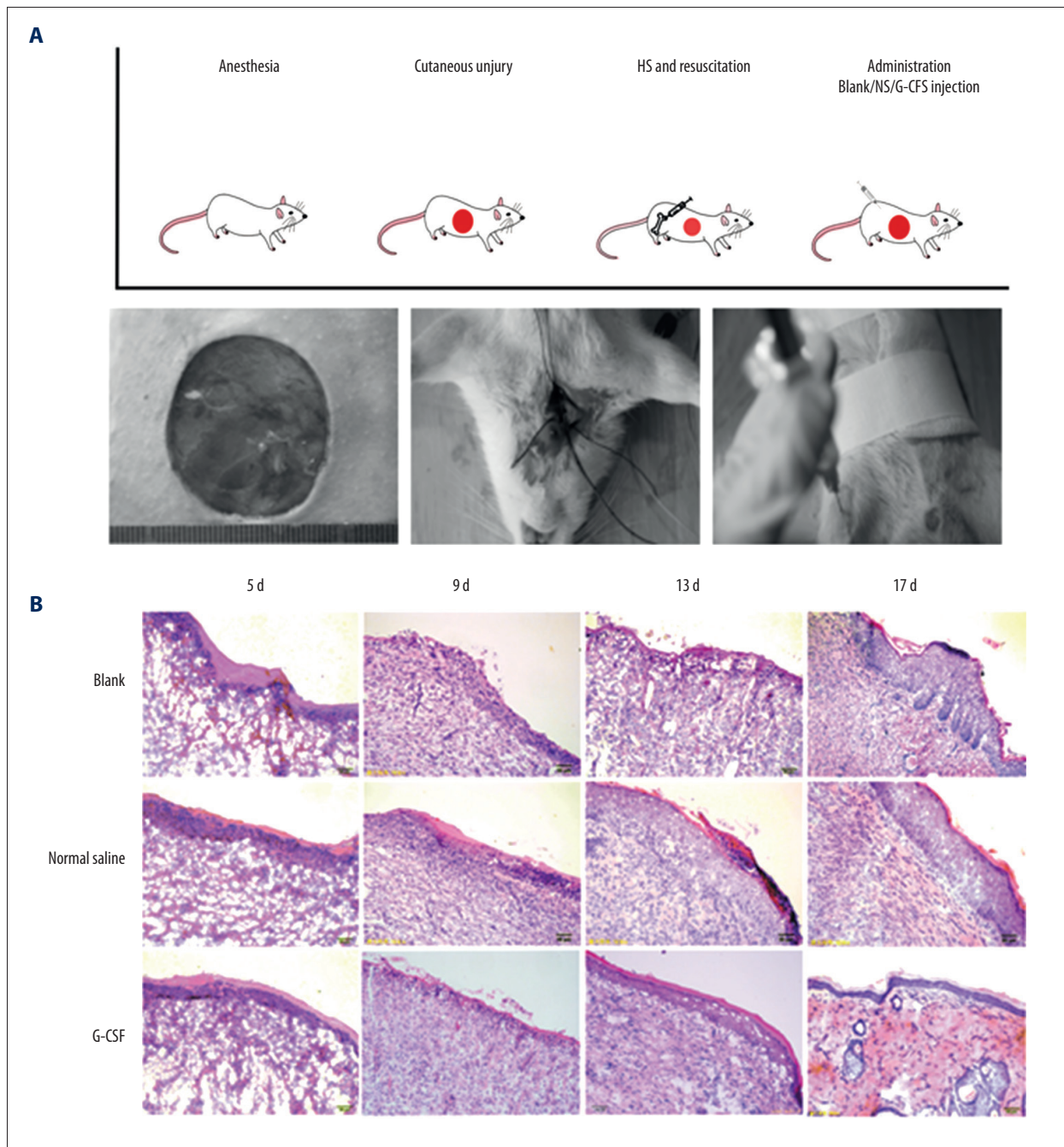
The results are depicted as mean  $\pm$ SD. The statistical comparisons used the paired Wilcoxon's test using SPSS 11.0 software

(SPSS, Inc., USA). P-value  $<0.05$  was considered to be statistically significant.

## Results

### G-CSF improved wound repair under hemorrhagic shock

The hemorrhagic shock combined with cutaneous injury rat model was established as shown in Figure 1A. The wounded



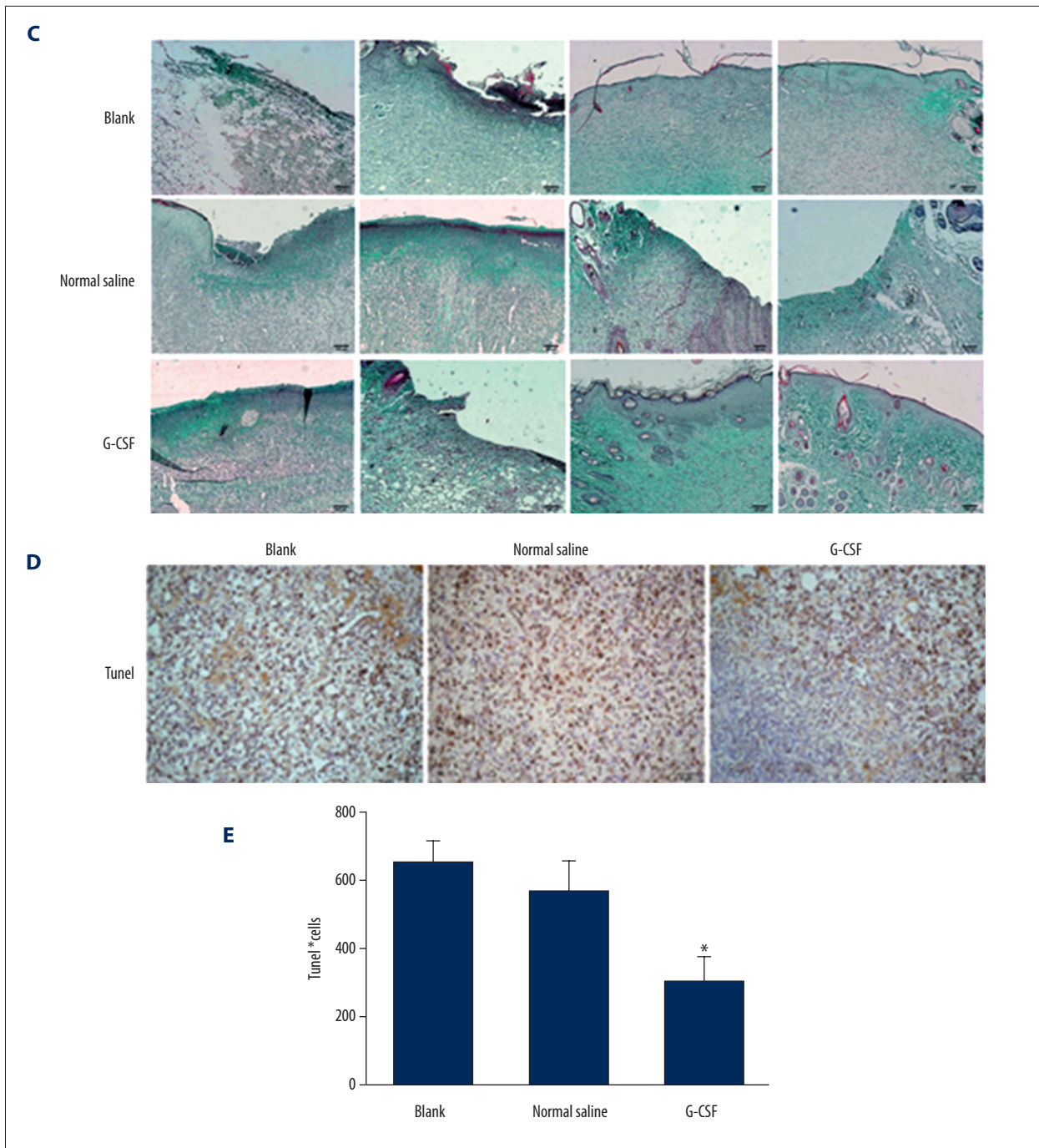


**Figure 1.** G-CSF improved wound healing in hemorrhagic shock. **(A)** The protocol of hemorrhagic shock combined with cutaneous injury model and resuscitation treatment. The rats underwent 3-cm-diameter full-thickness skin incision and 40% total blood loss for 60 min. The rats were resuscitated with a bolus of 4 mL/kg HHES infusion. After resuscitation, all the rats randomly received G-CSF, normal saline, or no treatment. H&E **(B)** and Masson trichrome **(C)** staining during wound repair. Scale bar=100  $\mu$ m. **(D)** G-CSF attenuated tissue apoptosis in wound areas by TUNEL assay. Scale bar=100  $\mu$ m. **(E)** The number of apoptosis cells in the wound skin. Ten pictures of each group were taken and calculated. Data are shown as mean  $\pm$ SD. \*  $P < 0.05$  versus blank group.

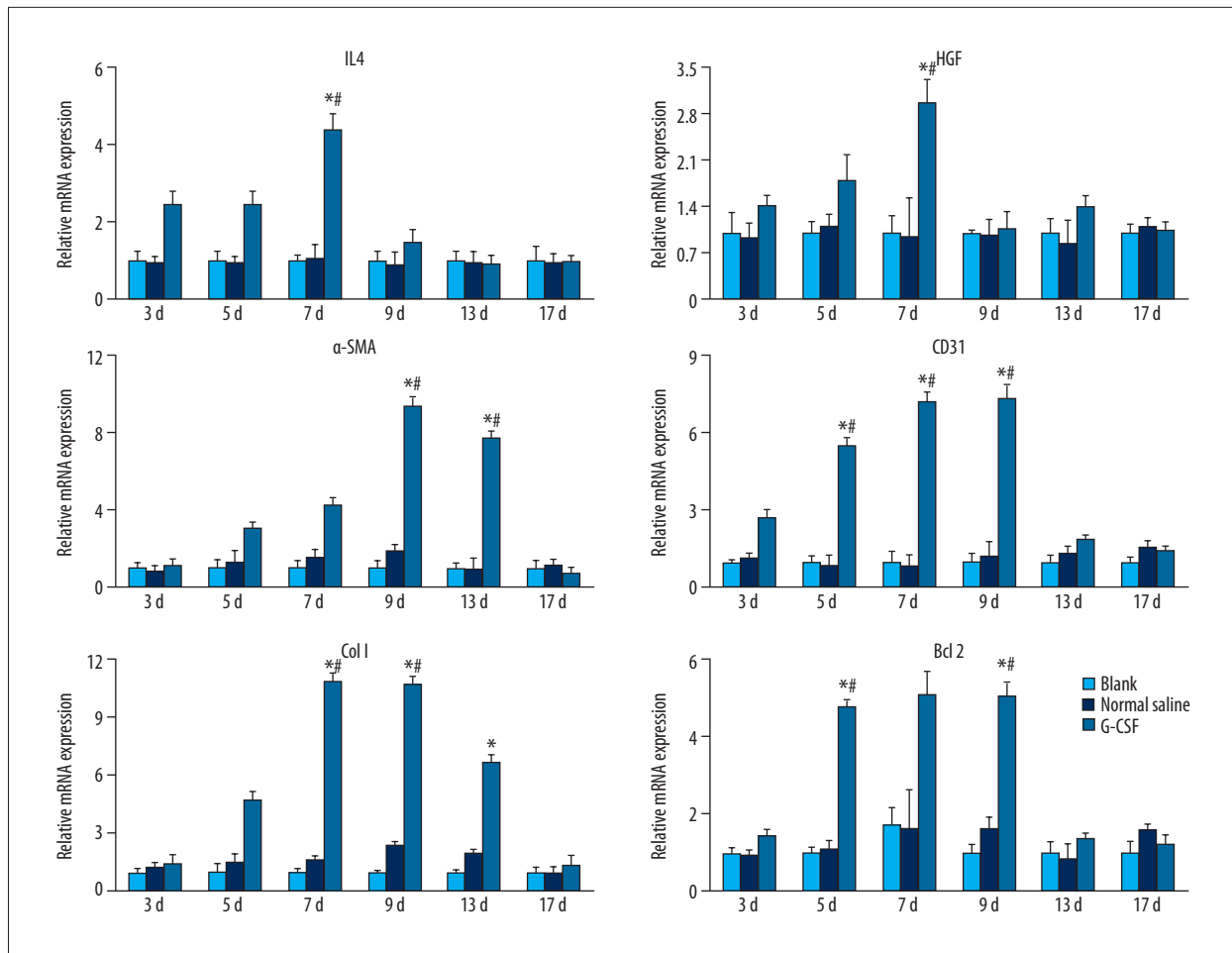


**Figure 2.** Wound healing-related mRNA modulation by G-CSF. Each result was repeated at least for 3 times. Data are shown as mean  $\pm$ SD. \*  $P < 0.05$  versus Blank group, #  $P < 0.05$  versus Normal saline group.

skin tissues were sectioned and stained with H&E and Masson trichrome (Figures 1B, 1C). The H&E staining results showed less inflammatory cells infiltration and earlier initiation of re-epithelialization in the G-CSF group on day 5. The G-CSF group exhibited more rapid epithelialization on day 9 and few cutaneous appendages such as follicular sebaceous units developed by day 17. Strong collagen staining with Masson trichrome suggested that the G-CSF-treated group initiated more rapid collagen synthesis and deposition after day 5, more homogeneous distribution by day 9, and continuously stable expression with complete healing by day 17. In addition, we analyzed the tissue apoptosis in the wounded skin by TUNEL staining (Figure 1D, 1E). The number of TUNEL-stained cells was significantly lower in the G-CSF group than in the normal saline group and blank group on day 9 ( $p < 0.05$ ). Thus, the anti-apoptotic effect on wounded skin was elevated in G-CSF compared to control groups. Collectively, these data suggest that G-CSF accelerated wound healing and ameliorated tissue apoptosis after fluid resuscitation in HS rats.

### G-CSF attenuated inflammation reaction, apoptotic events, and promoted angiogenesis in wound areas

Next, we examined the anti-inflammatory factors IL4, anti-apoptotic factor Bcl 2, collagen deposition-related factors collagen I and HGF, and angiogenesis-related factors CD31 and  $\alpha$ -SMA expression by RT-PCR (Figure 2). The quantification results implied that the anti-inflammatory factor IL 4 was significantly up-regulated since day 3. The angiogenesis-related factors, CD31 and  $\alpha$ -SMA, were up-regulated as early as day 5 and peaked at day 9. Collagen synthesis-related genes were modulated early to initiate the repair as well as collagen deposition in the remodeling stage, and we found an enhanced expression of collagen I genes from day 7 to day 13 in the G-CSF group. HGF expression was peaked at day 7. The expression of the anti-apoptotic Bcl 2 gene was up-regulated from day 5 to day 9 compared to control groups. The up-regulation of Bcl 2 in the G-CSF group was in agreement with lower TUNEL-positive cell numbers on day 9. Nevertheless, decreased anti-apoptotic gene and anti-inflammatory gene expressions would lead to chronic non-healing ulcer in control groups.

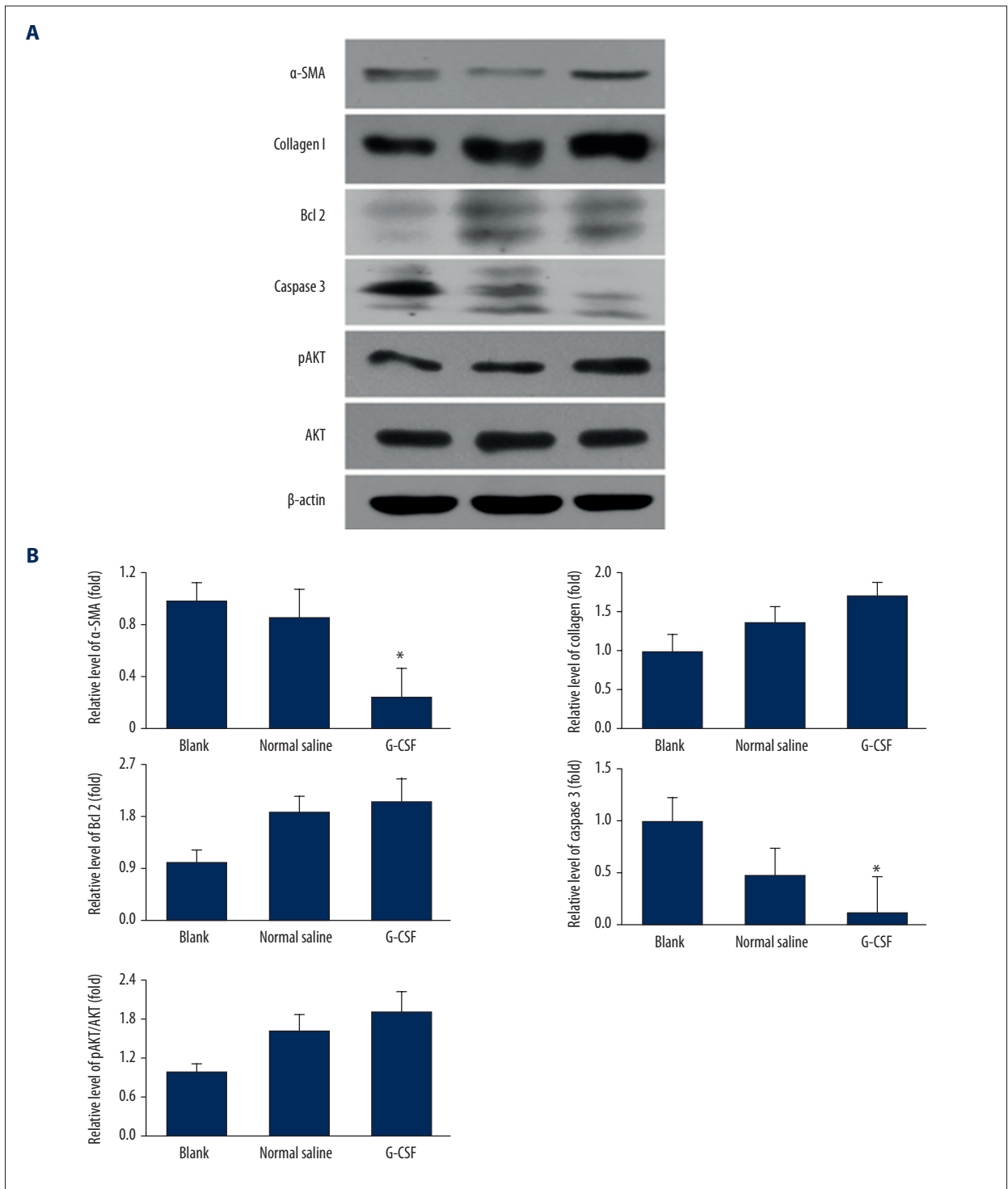


**Figure 3.** Protective effects of G-CSF on wound healing-related protein expression. **(A)**  $\alpha$ -SMA, Collagen I, Bcl 2, Caspase 3, pAKT, AKT,  $\beta$ -actin expressions were evaluated by WB. **(B)** Each protein was normalized by  $\beta$ -actin and showed as fold change of Blank group. Each result was repeated at least for 3 times. Data were shown as mean  $\pm$ SD. \*  $P < 0.05$  versus Blank group, #  $P < 0.05$  versus Normal saline group.

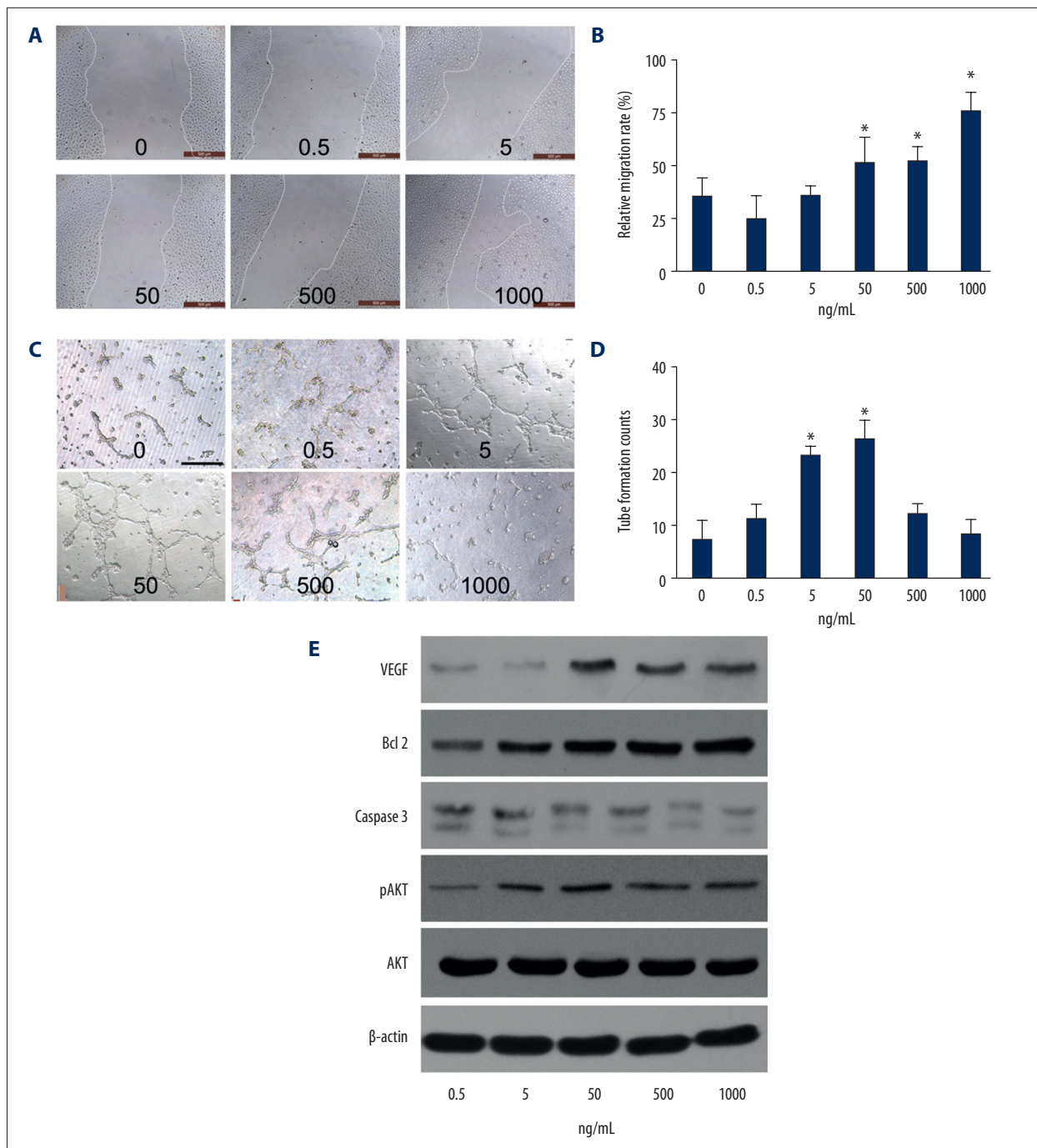


**Figure 4.** G-CSF promoted the angiogenic potential of HUVECs *in vitro*. **(A)** Representative images depicting the effect of the G-CSF treatment at 12 h on HUVEC migration at the indicated concentrations. **(B)** Statistically calculated relative migration rates; Scale bar=500  $\mu$ m. **(C)** Typical images of the tube-like structures in the presence of G-CSF cultured on Matrigel for 12 h. **(D)** The amounts of capillary-like structures; Scale bar=200  $\mu$ m. **(E)** Western blot of VEGF, Bcl 2, Caspase 3, phosphorylated AKT (pAKT) as well as the total AKT and  $\beta$ -actin expressions at different concentrations of G-CSF; the HUVECs were pre-incubated with G-CSF for 24 h then followed by  $H_2O_2$  stimulation (50  $\mu$ mol/L) to determine the protein activities by Western blot. Each experiment was repeated 3 times and typical pictures are shown. Data are shown as mean  $\pm$ SD. \*  $P < 0.05$  versus HUVECs without G-CSF stimulation.

We further investigated the protein expression of  $\alpha$ -SMA, collagen I, Bcl 2, caspase 3, AKT and pAKT post HS combined with cutaneous injury on 9 d (Figure 3A, 3B). The results indicated that G-CSF also enhanced angiogenesis, improved collagen synthesis and anti-apoptotic factors' expression at protein level and activated AKT signaling pathway.

### G-CSF exerted angiogenesis potential on HUVECs *in vitro*

To determine the effect of G-CSF treatment on the angiogenesis potential of ECs *in vitro*, we examined the migration and tube formation abilities of HUVECs at different concentration of G-CSF stimulation (0.5, 5, 50, 500, 1000 ng/mL) (Figure 4A, 4B). The scratch experiment showed that the migration ability of the HUVECs was enhanced significantly by G-CSF at 12 h in a concentration-dependent manner. The assay showed that tube formation ability of the HUVECs was promoted by G-CSF at 12 h and peaked at 50 ng/mL G-CSF (Figure 4C, 4D). In addition, H<sub>2</sub>O<sub>2</sub> was added into HUVECs for 6 h to mimic the apoptotic environment *in vivo*. VEGF, Bcl 2, caspase 3, AKT, and pAKT were evaluated by WB (Figure 4E). VEGF was increased in the G-CSF group and peaked at 50 ng/mL. Caspase 3 was decreased while Bcl 2 was more highly expressed with the higher concentration of G-CSF. The results are in accordance with mRNA modulation *in vivo*, in which G-CSF stimulated proliferation, maturation, and anti-apoptotic capacities of ECs.

## Discussion

Wound healing is one of the most complicated biological processes [1]. In the present study, we demonstrated that G-CSF administration after resuscitation is beneficial for wound healing under conditions of hemorrhagic shock by modulating inflammation, improving collagen deposition, and enhancing function of ECs.

The potential impacts of G-CSF on angiogenesis have attracted great scientific interest. A growing number of studies indicate that G-CSF has therapeutic effects on tissue repair and regeneration, including full-thickness skin injuries, burn injuries, limb ischemia, myocardial infarction, and pulmonary hypertension, by specifically enhancing the pro-angiogenic abilities of ECs [24–27]. Angiogenesis is also of importance to the adequate healing of vessels and microvessels by providing sufficient oxygen and necessary nutrients for cell growth and development [8]. This dynamic process is regulated by interaction of diverse cytokines, growth factors, and molecular signal pathways between different cell types [1,7]. Our results of mRNA expression in the G-CSF treated group *in vivo* showed up-regulated expression of IL 4, CD31,  $\alpha$ -SMA, and HGF in skin wound areas. The essential factors such as CD31 and  $\alpha$ -SMA were augmented to played critical roles in angiogenesis

at the inflammation and proliferative stage. *In vitro* experimentation in G-CSF-stimulated HUVECs show that the proliferative ECs and the enhanced vasculature contributed to angiogenesis and benefited wound healing. Additionally, it was previously demonstrated that EPCs are mobilized by G-CSF to damaged tissues and significantly promote angiogenesis by increasing the secretion of angiogenic cytokines in full-thickness incision, burned, and focal cerebral ischemia rats and myocardial infarcted rabbits [28–30]. Thus, G-CSF administration would be expected to play important roles in wound repair, partly by ameliorating inflammation and enhancing angiogenesis [31,32].

G-CSF was reported to protect tissue by strengthening anti-apoptotic effects of host cells under adverse conditions. In central nervous system (CNS) disease, G-CSF was suggested to inhibit neurocyte apoptosis and attenuated glutamate-induced cell death [24]. G-CSF displayed strong anti-apoptotic activity in mature nerve cells by activating multiple survival signaling mechanisms [33,34]. Several studies reported that G-CSF increased anti-inflammatory activities and facilitated neuron protective and angiogenesis effects [33,35,36]. Bcl-2 plays a vital role in the apoptosis signaling pathway. Our *in vivo* and *in vitro* experiments showed up-regulated Bcl 2 expression in the presence of G-CSF, which suggests the anti-apoptosis capacity was enhanced under injury circumstances. Initiation of apoptosis is one of the natural processes during wound healing. Among the effective approaches for cutaneous therapeutics, enhancing the survival of host cells promotes wound healing quality. In addition, it will be interesting to determine the interconnection between anti-apoptotic treatments and wound healing quality or prognosis, which may provide complementary information about wound repair combined with severe trauma. Future studies will attempt to better resolve the mechanisms by which G-CSF provokes the anti-apoptotic effect in tissue repair and regeneration.

## Conclusions

To summarize, we provided evidence for a cytoprotective and beneficial effect of G-CSF administration after resuscitation in a hemorrhagic shock combined with cutaneous injury rat model. Tissue damage was ameliorated and angiogenesis was significantly elevated to support tissue repair and regeneration by G-CSF administration. These findings uphold the suggestion that G-CSF administration would be beneficial for patients in cutaneous therapy, even in hemorrhagic shock.

### Conflict of interests

The authors have no conflict of interest to declare.

## References:

1. Gurtner GC, Werner S, Barrandon Y, Longaker MT: Wound repair and regeneration. *Nature*, 2008; 453: 314–21
2. Wong VW, Akaishi S, Longaker MT, Gurtner GC: Pushing back: Wound mechanotransduction in repair and regeneration. *J Invest Dermatol*, 2011; 131: 2186–96
3. Broughton G 2nd, Janis JE, Attinger CE: Wound healing: An overview. *Plast Reconstruct Surg*, 2006; 117: 1e–S–32e–S
4. McGinn FP: Proceedings: Effect of haemorrhage on wound healing in the rat. *Br J Surg*, 1976; 63: 163
5. Bjerkvig CK, Strandenes G, Eliassen HS et al: “Blood failure” time to view blood as an organ: how oxygen debt contributes to blood failure and its implications for remote damage control resuscitation. *Transfusion*, 2016; 56(Suppl.) 2: S182–89
6. Eltzschig HK, Eckle T: Ischemia and reperfusion – from mechanism to translation. *Nat Med*, 2011; 17: 1391–401
7. Keel M, Trentz O: Pathophysiology of polytrauma. *Injury*, 2005; 36: 691–709
8. Eming SA, Martin P, Tomic-Canic M: Wound repair and regeneration: Mechanisms, signaling, and translation. *Sci Transl Med*, 2014; 6: 265sr6
9. Layman H, Sacasa M, Murphy AE et al: Co-delivery of FGF-2 and G-CSF from gelatin-based hydrogels as angiogenic therapy in a murine critical limb ischemic model. *Acta Biomater*, 2009; 5: 230–39
10. Zhang Y, Adachi Y, Iwasaki M et al: G-CSF and/or M-CSF accelerate differentiation of bone marrow cells into endothelial progenitor cells *in vitro*. *Oncol Rep*, 2006; 15: 1523–27
11. Takahashi T, Kalka C, Masuda H et al: Ischemia- and cytokine-induced mobilization of bone marrow-derived endothelial progenitor cells for neovascularization. *Nat Med*, 1999; 5: 434–38
12. Bussolino F, Wang JM, Defilippi P et al: Granulocyte- and granulocyte-macrophage-colony stimulating factors induce human endothelial cells to migrate and proliferate. *Nature*, 1989; 337: 471–73
13. Lee M, Aoki M, Kondo T et al: Therapeutic angiogenesis with intramuscular injection of low-dose recombinant granulocyte-colony stimulating factor. *Arterioscler Thromb Vasc Biol*, 2005; 25: 2535–41
14. Chen CH, Sereti KI, Wu BM, Ardehali R: Translational aspects of cardiac cell therapy. *J Cell Mol Med*, 2015; 19: 1757–72
15. Shi Q, Hodara V, Butler SD et al: Differential bone marrow stem cell mobilization by G-CSF injection or arterial ligation in baboons. *J Cell Mol Med*, 2009; 13: 1896–906
16. Tateishi-Yuyama E, Matsubara H, Murohara T et al: Therapeutic angiogenesis for patients with limb ischaemia by autologous transplantation of bone-marrow cells: A pilot study and a randomised controlled trial. *Lancet*, 2002; 360: 427–35
17. Moazzami K, Moazzami B, Roohi A et al: Local intramuscular transplantation of autologous mononuclear cells for critical lower limb ischaemia. *Cochrane Database Syst Rev*, 2014; (12): CD008347
18. Schabitz WR, Kollmar R, Schwaninger M et al: Neuroprotective effect of granulocyte colony-stimulating factor after focal cerebral ischemia. *Stroke*, 2003; 34: 745–51
19. Nakayama H, Iohara K, Hayashi Y et al: Enhanced regeneration potential of mobilized dental pulp stem cells from immature teeth. *Oral Dis*, 2016 [Epub ahead of print]
20. Wu X, Yang S, Wang H et al: G-CSF/SCF exert beneficial effects via anti-apoptosis in rabbits with steroid-associated osteonecrosis. *Exp Mol Pathol*, 2013; 94: 247–54
21. Lan X, Qu H, Yao W, Zhang C: Granulocyte-colony stimulating factor inhibits neuronal apoptosis in a rat model of diabetic cerebral ischemia. *Tohoku J Exp Med*, 2008; 216: 117–26
22. Pitzer C, Klussmann S, Kruger C et al: The hematopoietic factor granulocyte-colony stimulating factor improves outcome in experimental spinal cord injury. *J Neurochem*, 2010; 113: 930–42
23. Huang H, Liu J, Hao H et al: G-CSF Administration after the intraosseous infusion of hypertonic hydroxyethyl starches accelerating wound healing combined with hemorrhagic shock. *BioMed Res Int*, 2016; 2016: 5317630
24. Strecker JK, Sevimli S, Schilling M et al: Effects of G-CSF treatment on neutrophil mobilization and neurological outcome after transient focal ischemia. *Exp Neurol*, 2010; 222: 108–13
25. Tanaka R, Masuda H, Kato S et al: Autologous G-CSF-mobilized peripheral blood CD34+ cell therapy for diabetic patients with chronic nonhealing ulcer. *Cell Transpl*, 2014; 23: 167–79
26. Kang J, Yun JY, Hur J et al: Erythropoietin priming improves the vasculogenic potential of G-CSF mobilized human peripheral blood mononuclear cells. *Cardiovasc Res*, 2014; 104: 171–82
27. Liu JF, Du ZD, Chen Z et al: Granulocyte colony-stimulating factor attenuates monocrotaline-induced pulmonary hypertension by upregulating endothelial progenitor cells via the nitric oxide system. *Exp Ther Med*, 2013; 6: 1402–8
28. Fox A, Smythe J, Fisher N et al: Mobilization of endothelial progenitor cells into the circulation in burned patients. *Br J Surg*, 2008; 95: 244–51
29. Minatoguchi S, Takemura G, Chen XH et al: Acceleration of the healing process and myocardial regeneration may be important as a mechanism of improvement of cardiac function and remodeling by postinfarction granulocyte colony-stimulating factor treatment. *Circulation*. 2004; 109: 2572–80
30. Lee ST, Chu K, Jung KH et al: Granulocyte colony-stimulating factor enhances angiogenesis after focal cerebral ischemia. *Brain Res*, 2005; 1058: 120–28
31. Agalar F, Iskit AB, Agalar C et al: The effects of G-CSF treatment and starvation on bacterial translocation in hemorrhagic shock. *J Surg Res*, 1998; 78: 143–47
32. Ghannam S, Bouffi C, Djouadi F et al: Immunosuppression by mesenchymal stem cells: Mechanisms and clinical applications. *Stem Cell Res Ther*, 2010; 1: 2
33. Schneider A, Kruger C, Steigleder T et al: The hematopoietic factor G-CSF is a neuronal ligand that counteracts programmed cell death and drives neurogenesis. *J Clin Invest*, 2005; 115: 2083–98
34. Komine-Kobayashi M, Zhang N, Liu M et al: Neuroprotective effect of recombinant human granulocyte colony-stimulating factor in transient focal ischemia of mice. *J Cereb Blood Flow Metab*, 2006; 26(3): 402–13
35. Sehara Y, Hayashi T, Deguchi K et al: Decreased focal inflammatory response by G-CSF may improve stroke outcome after transient middle cerebral artery occlusion in rats. *J Neurosci Res*, 2007; 85: 2167–74
36. Solaroglu I, Cahill J, Tsubokawa T et al: Granulocyte colony-stimulating factor protects the brain against experimental stroke via inhibition of apoptosis and inflammation. *Neurol Res*, 2009; 31: 167–72